Spontaneous radiative decay of translational levels of an atom near a dielectric surface

Fam Le Kien* and K. Hakuta

Department of Applied Physics and Chemistry, University of Electro-Communications, Chofu, Tokyo 182-8585, Japan

(Received 11 September 2006; revised manuscript received 12 December 2006; published 30 January 2007)

We study spontaneous radiative decay of translational levels of an atom in the vicinity of a semi-infinite dielectric. We systematically derive the microscopic dynamical equations for the spontaneous decay process. We calculate analytically and numerically the radiative linewidths and the spontaneous transition rates for the translational levels. The roles of the interference between the emitted and reflected fields and of the transmission into the evanescent modes are clearly identified. Our numerical calculations for the silica-cesium interaction show that the radiative linewidths of the bound excited levels with large enough but not too large vibrational quantum numbers are moderately enhanced by the emission into the evanescent modes and those for the deep bound levels are substantially reduced by the surface-induced redshift of the transition frequency.

DOI: 10.1103/PhysRevA.75.013423 PACS number(s): 42.50.Vk, 32.80.−t, 32.70.Jz

I. INTRODUCTION

Due to recent progress in atom optics and nanotechnology, the study of individual neutral atoms in the vicinities of material surfaces has gained renewed interest [1–5]. A method for microscopic trapping and guiding individual atoms along a nanofiber has been proposed [1]. An optical technique for loading atoms into quantum adsorption states of a dielectric surface has been suggested [2,3]. An effective transfer of optical energy to kinetic energy has been demonstrated [6]. The possibility to control and manipulate individual atoms near surfaces can find applications for quantum information [7–9] and atom chips [10,11]. Cold atoms can be used as a probe that is very sensitive to surface-induced perturbations [12]. Many applications require a deep understanding and an effective control of spontaneous emission. However, a systematic microscopic theory for spontaneous radiative decay of an atom moving in a confining potential is still missing.

It is well known that the spontaneous emission rate of an atom is modified by the presence of an interface [13–20]. Such a phenomenon has been demonstrated experimentally [13]. A semiclassical approach to the problem of surface-modified radiative properties has been presented [14]. A quantum-mechanical linear-response formalism has been developed for an atom close to an arbitrary interface [15–17]. An alternative approach based on the mode expansion has been used for an atom near a perfect conductor [18] or a dielectric [19]. A quantum treatment for the internal dynamics of a multilevel atom near a multilayered dielectric medium has been performed [20]. In previous treatments [14–20], the effect of the center-of-mass motion of the atom on the spontaneous emission process was neglected. In this condition, the effects of the surface on the spontaneous radiative decay of the atom manifest simply as a quantum electrodynamic enhancement due to the mode modification and a frequency shift due to the surface-atom van der Waals interaction, with no change in the level structure [16,17].

Lately translational levels of an atom in a surface-induced potential have been studied [2,3]. An experimental observation of the excitation spectrum of cesium atoms in quantum adsorption states of a nanofiber surface has been reported [21]. In the theoretical treatments of Refs. [2,3], the quantum electrodynamic enhancement of spontaneous emission due to the mode modification was completely neglected and a set of equations with phenomenologically added decay terms was used for describing the dynamics of the loading process. A more rigorous theory requires a deeper knowledge of the structure of the decay equations and the magnitudes of the decay coefficients for the translational levels of the atom.

In this paper, we study spontaneous radiative decay of translational levels of an atom in the vicinity of a semi-infinite dielectric. Our study is general in the sense that it incorporates the quantum nature of the radiation field in the presence of the dielectric as well as the quantum center-of-mass motion of the atom. We systematically derive the microscopic dynamical equations for the spontaneous decay process, which reflect the complexity of the translational levels of the atom in the potential. We focus our attention on the radiative linewidths and the spontaneous transition rates. Our results obtained by the quantum mode-expansion approach allow us to identify the roles of the interference between the emitted and reflected fields and of the transmission into the evanescent modes. Our formalism and analytical results are, in principle, applicable to any confining potential for the center-of-mass motion. As an example, we pick a particular model for the surface-atom potential and present numerical results pertaining to the radiative decay rates.

The paper is organized as follows. In Sec. II we describe the model. In Sec. III we derive the basic dynamical equations for the spontaneous radiative decay process. In Sec. IV we study analytically the decay rates. In Sec. V we present the results of numerical calculations. Our conclusions are given in Sec. VI.

II. MODEL

We consider a space with one interface. The half-space $x<0$ is occupied by a nondispersive nonabsorbing dielectric medium (medium 1). The half-space $x>0$ is occupied by

*Also at Institute of Physics and Electronics, Vietnamese Academy of Science and Technology, Hanoi, Vietnam.

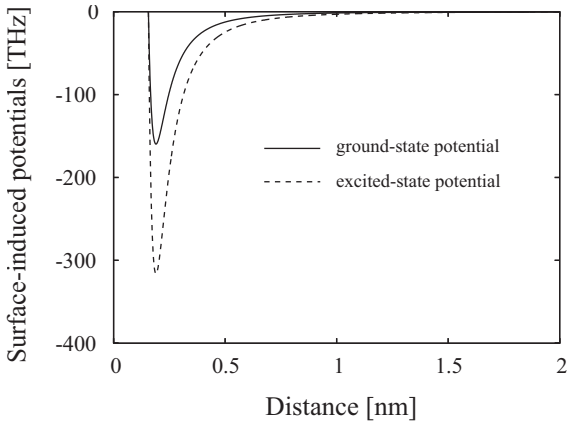

FIG. 1. Surface-induced potentials for ground- and excited-state atoms. The parameters are $C_{3g}=1.56$ kHz μm^3, $C_{3e}=3.09$ kHz μm^3, $A_g=1.6\times10^{18}$ Hz, $A_e=3.17\times10^{18}$ Hz, and $\alpha_g=\alpha_e=53$ nm^{-1}. They are taken for the case of a D_2-line cesium atom in the vicinity of a semi-infinite silica medium.

vacuum (medium 2). We examine an atom, with an upper internal level e and a lower internal level g, moving in the empty half-space $x>0$. The energies of the internal levels e and g are denoted by $\hbar\omega_e$ and $\hbar\omega_g$, respectively.

A. Quantum translational states of the atom

We consider the quantum center-of-mass motion of the atom in a confining potential induced by the surface-atom interaction. Despite a large volume of research on the surface-atom interaction, due to the complexity of surface physics and the lack of data, the actual form of the potential is yet to be ascertained [22]. For the purpose of numerical demonstration of our formalism, we choose the following model for the potential [2,22]:

$$V_j(x)=A_je^{-\alpha_jx}-\frac{C_{3j}}{x^3}. \tag{1}$$

Here, $j=e$ or g labels the internal state of the atom, C_{3j} is the van der Waals coefficient, and A_j and α_j determine the height and range, respectively, of the short-range repulsion. Note that the potential (1) depends on the internal state j of the atom (see Fig. 1).

The potential parameters C_{3j}, A_j, and α_j depend on the dielectric and the atom. In numerical calculations, we use the parameters of fused silica, for the dielectric, and the parameters of atomic cesium with the D_2 line, for the two-level atomic model. The refractive index of fused silica is $n_1=1.45$, the mass of atomic cesium is $m=132.9$ a.u., and the free-space wavelength of the cesium D_2 line is $\lambda_0=852$ nm. In Appendix A, the parameters of the ground- and excited-state potentials for the silica-cesium interaction are estimated to be $C_{3g}=1.56$ kHz μm^3, $C_{3e}=3.09$ kHz μm^3, $A_g=1.6\times10^{18}$ Hz, $A_e=3.17\times10^{18}$ Hz, and $\alpha_g=\alpha_e=53$ nm^{-1}. The potential depths are $D_g=159.6$ THz and $D_e=316$ THz. The minimum positions for both potentials are assumed to be the same, equal to $x_m=0.19$ nm.

The ground-state van der Waals coefficient $C_{3g}=1.56$ kHz μm^3 was extrapolated from the result of Ref. [23] for the interaction between a ground-state cesium atom and a perfect metal surface. The excited-state van der Waals coefficient $C_{3e}=3.09$ kHz μm^3 was obtained as a result of the assumption $C_{3e}/C_{3g}=1.98$ for cesium. This ratio was inferred from the results of Ref. [24] (see also [25]), where the core contributions were neglected. The huge repulsive amplitude $A_g=1.6\times10^{18}$ Hz and the large decay coefficient $\alpha_g=53$ nm^{-1} were chosen because, when combined with the van der Waals coefficient $C_{3g}=1.56$ kHz μm^3, they lead to a ground-state potential V_g with depth equal to the experimental value $D_g=0.66$ eV$=159.6$ THz [26]. Because of the lack of data for the excited-state potential parameters, we have assumed that $A_e/A_g=D_e/D_g=C_e/C_g$ and $\alpha_e=\alpha_g$. Due to this assumption, the potentials for the excited and ground states look homothetic.

We emphasize that, due to the interplay between the repulsive part and the van der Waals part, the distance at which the combined potential V_g goes down to the minimum is $x_m=0.19$ nm, which is one order of magnitude different from the value $\alpha_g^{-1}=0.019$ nm. We note that, although the depth $D_e=316$ THz of the excited-state potential is huge, it is still smaller than the energy separation $\omega_{eg}\cong352$ THz between the excited and ground internal states, thus avoiding the level crossing problem. For higher electronic levels, since the surface-atom interaction quickly increases with increasing atomic excitation [24,27], level crossing may occur at small atom-surface distances. In this regime, the atomic model with two internal levels breaks down and, consequently, a multilevel description is required. Such an issue is beyond the scope of our present paper.

It is pertinent to make a few comments regarding the applicability of Eq. (1) as a suitable model for the surface-atom interaction. There is a lot of controversy regarding the shape of the potential. For example, the review by Hoinkes [22] mentioned eight different potential shapes for the surface-atom interaction, including the one given by Eq. (1). Even very recently, a simple potential like the Morse potential has been used to explain many of the physical aspects [3]. The parameters of a given form of the potential can be obtained by fitting the calculated and experimental values of observable quantities such as the intensities of diffracted atomic beams, the depth and range of the potential, and the energy levels. The focus of the debate is the shape and the range of the repulsive potential since very little experimental and theoretical data are available at small distances.

The theoretical justification of the potential (1) was the asymptotic behavior of an atom very near to or away from the surface [2,22]. This particular form is a superposition of the two dependences: the short-range repulsive potential and the long-range attractive van der Waals potential. It is clear that, when the atom is very close to the surface, the discrete structure of the solid cannot be neglected. Due to the broken translational symmetry at the surface, the external fields can couple to the surface excitations with different wave vectors. Therefore, the surface-atom interaction becomes nonlocal at short distances. The nonlocal response may lead to spatial dispersion which in principle should be accounted for in estimating the fields reflected from or transmitted through the surface and, consequently, in calculating the van der Waals interaction [28]. In addition, the van der Waals coefficient C_3

varies with the distance of the atom from the surface because of the distance-dependent influence of the electronic core transitions [29]. However, we neglect such effects.

Keeping the aforesaid in view, we ignore all the details of the surface assuming the translational invariance to be valid. Moreover, we model the surface-atom interaction by Eq. (1) since we are not aware of any better approximation for the same interaction. Another important issue is the sensitivity of the results to the parameters of the repulsive potential. Calculations in this direction carried out by Lima *et al.* [2] show the robustness of the results against variations of the repulsive potential parameters. According to their calculations, a change by a factor of 10^4 in A or by a factor of 5 in α practically does not affect the vibrational levels that are close to the dissociation limit. Such shallow levels are mainly determined by the van der Waals part of the potential.

The Hamiltonian of the atom in the surface-induced potential is given by

$$H_A = \frac{p^2}{2m} + \sum_{j=e,g} [\hbar\omega_j + V_j(x)]|j\rangle\langle j|. \tag{2}$$

Here, p and m are the momentum and mass of the atom, respectively, and ω_j is the frequency of the internal level j. We introduce the notation $|\varphi_a\rangle$ and $|\varphi_b\rangle$ for the eigenstates of the center-of-mass motion of the atom in the potentials $V_e(x)$ and $V_g(x)$, respectively. The wave functions $\varphi_a(x)$ and $\varphi_b(x)$ are determined by the stationary Schrödinger equations

$$\left[-\frac{\hbar^2}{2m}\frac{d^2}{dx^2} + V_e(x)\right]\varphi_a(x) = \mathcal{E}_a\varphi_a(x),$$

$$\left[-\frac{\hbar^2}{2m}\frac{d^2}{dx^2} + V_g(x)\right]\varphi_b(x) = \mathcal{E}_b\varphi_b(x), \tag{3}$$

respectively. The eigenvalues $\mathcal{E}_a$ and $\mathcal{E}_b$ characterize the energies of the translational levels of the excited and ground states, respectively. Without loss of generality, we assume that the center-of-mass eigenfunctions φ_a and φ_b are real functions.

We introduce the combined eigenstates $|a\rangle = |e\rangle \otimes |\varphi_a\rangle$ and $|b\rangle = |g\rangle \otimes |\varphi_b\rangle$, which are formed from the internal and translational eigenstates. The corresponding energies are $\hbar\omega_a = \hbar\omega_e + \mathcal{E}_a$ and $\hbar\omega_b = \hbar\omega_g + \mathcal{E}_b$. Then, we can represent the Hamiltonian (2) in the diagonal form $H_A = \Sigma_a \hbar\omega_a|a\rangle\langle a| + \Sigma_b \hbar\omega_b|b\rangle\langle b|$. We emphasize that the summations over a and b include both the discrete ($\mathcal{E}_{a,b} < 0$) and continuous ($\mathcal{E}_{a,b} > 0$) spectra. The levels a with $\mathcal{E}_a < 0$ and the levels b with $\mathcal{E}_b < 0$ are called the bound (or vibrational) levels of the excited and ground states, respectively. In such a state, the atom is bound to the surface. It is vibrating or, more exactly, moving back and forth between the walls formed by the van der Waals potential and the repulsion potential. The levels a with $\mathcal{E}_a > 0$ and the levels b with $\mathcal{E}_b > 0$ are called the free (or continuum) levels of the excited and ground states, respectively. The center-of-mass wave functions of the bound levels are normalized to unity. The center-of-mass wave functions of the free levels are normalized per unit energy. For bound states, the center-of-mass wave functions φ_a and φ_b can be labeled by the quantum numbers ν_a and ν_b, respectively. For free levels, the conventional sums over a and b must be replaced by the integrals over $\mathcal{E}_a$ and $\mathcal{E}_b$, respectively.

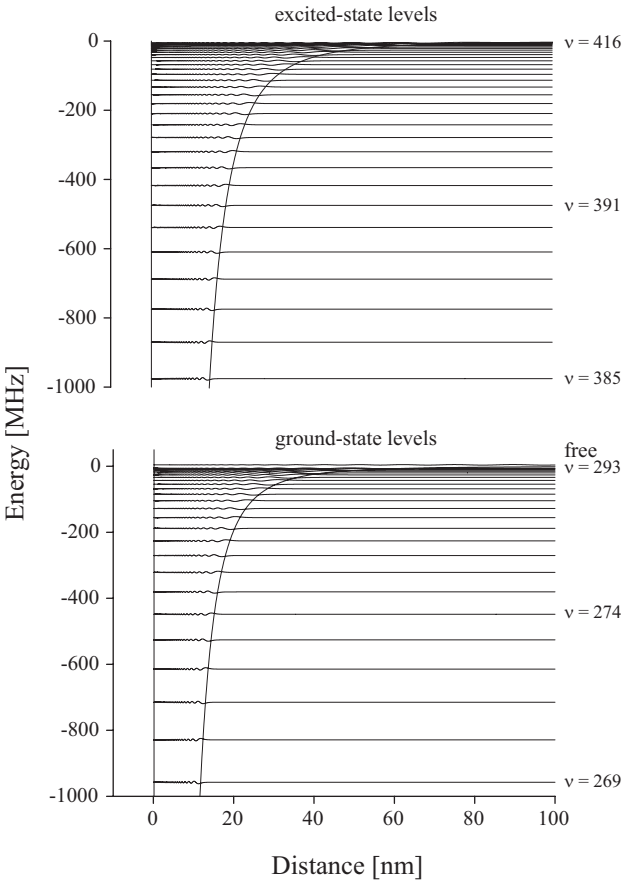

FIG. 2. Energies and wave functions of the center-of-mass motion of the ground- and excited-state atoms in the surface-induced potentials. The parameters of the potentials are as in Fig. 1. The mass of atomic cesium, $m = 132.9$ a.u., is used. We plot only the bound levels of the ground and excited states with energies in the range from -1 GHz to -5 MHz and the free ground-state level with energy of about 4.25 MHz.

The center-of-mass wave functions with energies in the range from -1 GHz to -5 MHz are plotted in Fig. 2. The center-of-mass eigenvalues in the range from -1 GHz to -20 kHz are displayed in Fig. 3. Note that the energy levels in the above range are very high compared to the depths $D_e = 316$ THz and $D_g = 159.6$ THz of the potentials V_e and V_g, respectively. Therefore, the corresponding wave functions are mainly determined by the long-range van der Waals interaction [2]. We find that the maximum quantum numbers for the excited- and ground-state potentials are 437 and 311, respectively. When the vibrational quantum number ν is small—that is, when the translational energy level $\mathcal{E}_\nu$ is deep—the wave function φ_ν depends strongly on the short-range repulsion (see Fig. 4). For such bound states, the center-of-mass wave functions are well confined to the proximity of the surface and the surface-induced frequency shifts of the atomic transitions are substantial compared to the optical frequency $\omega_0 = \omega_e - \omega_g \cong 352$ THz of the cesium D_2 line (see Figs. 4 and 5).

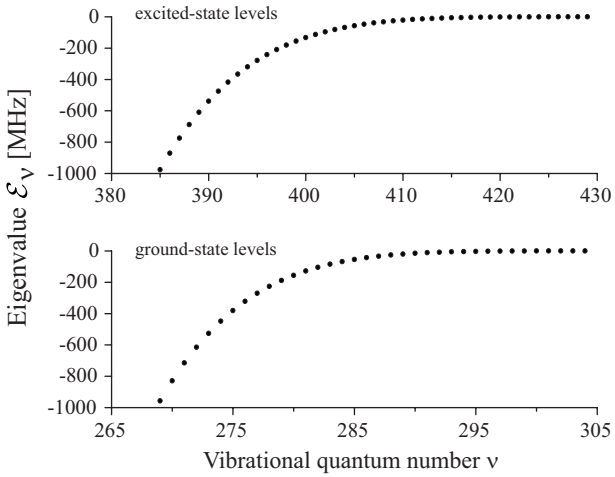

FIG. 3. Eigenvalues for the bound levels of the ground and excited states of the atom in the range from −1 GHz to −20 kHz. The parameters used are as for Fig. 2.

In the remaining part of this paper, we study the radiative properties of the translational levels. Before we proceed, we note that one of the main mechanisms of the relaxation to deeper translational levels of the surface-atom potential is the interaction with the surface phonons of the solid [30,31]. We also note that, due to surface-polariton modes [17,32,33], some energy transfer between different internal states may occur for very small atom-surface distances. We do not consider such nonradiative decay mechanisms in this paper.

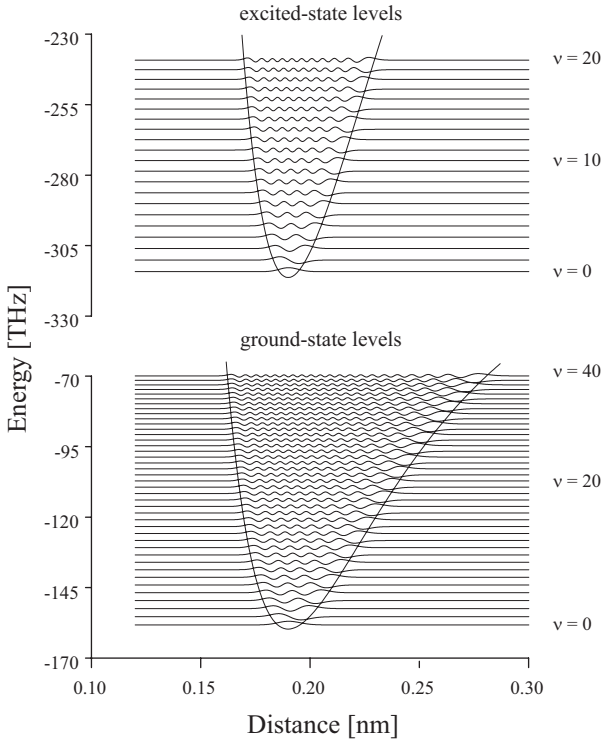

FIG. 4. Same as Fig. 2 but for the 21 lowest levels of the excited state and the 41 lowest levels of the ground state.

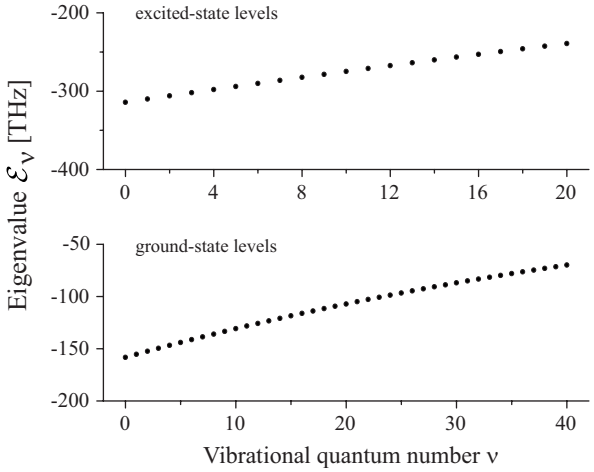

FIG. 5. Same as Fig. 3 but for the 21 lowest levels of the excited state and the 41 lowest levels of the ground state.

B. Quantum radiation field and its interaction with the atom

We use the formalism of Ref. [34] to describe the quantum radiation field in the space with one interface. We label the modes of the field by the index $\mu=(\omega\mathbf{K}qj)$, where ω is the mode frequency, $\mathbf{K}=(0,k_y,k_z)$ is the wave-vector component in the surface plane, $q=s,p$ is the mode polarization, and $j=1,2$ stands for the medium of the input. For each mode $\mu=(\omega\mathbf{K}qj)$, the condition $K\leqslant kn_j$ must be satisfied. Here, $k=\omega/c$ is the wave number in free space, $n_1>1$ is the refractive index of the dielectric, and $n_2=1$ is the refractive index of the vacuum. We neglect the dependence of the dielectric refractive index n_1 on the frequency and the wave number, like the previous works [14–20]. The neglect of spatial dispersion means the use of a local picture for the dielectric response. This local picture is not consistent with the nonlocal nature of the repulsive part of the potential. However, we expect that this inconsistency does not affect much the underlying physics of atomic translational levels, especially those levels which are close to the dissociation limit.

The mode functions are given, for $x<0$, by [34]

$$\mathbf{U}_{\omega\mathbf{K}s1}(x)=(e^{i\beta_1 x}+e^{-i\beta_1 x}r_{12}^{s})\hat{\mathbf{s}},$$

$$\mathbf{U}_{\omega\mathbf{K}p1}(x)=e^{i\beta_1 x}\hat{\mathbf{p}}_{1+}+e^{-i\beta_1 x}r_{12}^{p}\hat{\mathbf{p}}_{1-},$$

$$\mathbf{U}_{\omega\mathbf{K}s2}(x)=e^{-i\beta_1 x}t_{21}^{s}\hat{\mathbf{s}},$$

$$\mathbf{U}_{\omega\mathbf{K}p2}(x)=e^{-i\beta_1 x}t_{21}^{p}\hat{\mathbf{p}}_{1-}, \tag{4}$$

and, for $x>0$, by

$$\mathbf{U}_{\omega\mathbf{K}s1}(x)=e^{i\beta_2 x}t_{12}^{s}\hat{\mathbf{s}},$$

$$\mathbf{U}_{\omega\mathbf{K}p1}(x)=e^{i\beta_2 x}t_{12}^{p}\hat{\mathbf{p}}_{2+},$$

$$\mathbf{U}_{\omega\mathbf{K}s2}(x)=(e^{-i\beta_2 x}+e^{i\beta_2 x}r_{21}^{s})\hat{\mathbf{s}},$$

$$\mathbf{U}_{\omega\mathbf{K}p2}(x) = e^{-i\beta_2 x}\hat{\mathbf{p}}_{2-} + e^{i\beta_2 x} r_{21}^{p}\hat{\mathbf{p}}_{2+}. \quad (5)$$

In Eqs. (4) and (5), the quantity $\beta_j=(k^2n_j^2-K^2)^{1/2}$, with Re $\beta_j \geqslant 0$ and Im $\beta_j \geqslant 0$, is the magnitude of the x component of the wave vector in the medium j. The quantities $r_{ij}^{s}=(\beta_i-\beta_j)/(\beta_i+\beta_j)$ and $t_{ij}^{s}=2\beta_i/(\beta_i+\beta_j)$ are the reflection and transmission Fresnel coefficients for a TE mode, while the quantities $r_{ij}^{p}=(\beta_i n_j^2-\beta_j n_i^2)/(\beta_i n_j^2+\beta_j n_i^2)$ and $t_{ij}^{p}=2n_i n_j\beta_i/(\beta_i n_j^2+\beta_j n_i^2)$ are the reflection and transmission Fresnel coefficients for a TM mode. The vector $\hat{\mathbf{s}}=[\hat{\mathbf{K}}\times\hat{\mathbf{x}}]$ is the unit vector for the electric field in a TE mode, while the vectors $\hat{\mathbf{p}}_{j'\pm}=(K\hat{\mathbf{x}}\mp\beta_{j'}\hat{\mathbf{K}})/kn_{j'}$ are the unit vectors for the rightward- and leftward-propagating components of the electric field in a TM mode in the medium j'.

Note that a light beam propagating from the dielectric to the interface may be totally reflected because $n_1>n_2=1$. This phenomenon occurs for the modes $\mu=(\omega\mathbf{K}qj)$ with $j=1$ and $k<K\leqslant kn_1$. For such a mode, the magnitude of the x component of the wave vector in medium 2 is $\beta_2=i\sqrt{K^2-k^2}$, an imaginary number. This mode does not propagate in the x direction in the vacuum side of the interface but decays exponentially. Such a mode is an evanescent mode.

The total quantized electric field is given by [34]

$$\mathbf{E}(\mathbf{r}) = i\sum_{\mu}\frac{k}{4\pi}\sqrt{\frac{\hbar}{\pi\epsilon_0\beta_j}}e^{i\mathbf{K}\cdot\mathbf{R}}\mathbf{U}_{\mu}(x)a_{\mu}e^{-i\omega t} + \text{H.c.}, \quad (6)$$

where a_μ is the photon operator for the mode μ and $\Sigma_\mu=\Sigma_{qj}\int_0^\infty d\omega\int_0^{kn_j}KdK\int_0^{2\pi}d\phi$ is the generalized summation over the modes. Here, ϕ is the azimuthal angle of the vector $\mathbf{K}$ in the yz plane. The commutation rule for the photon operators is $[a_\mu,a_{\mu'}^{\dagger}]=\delta(\omega-\omega')\delta(\mathbf{K}-\mathbf{K}')\delta_{qq'}\delta_{jj'}$. When dispersion in the region around the frequencies of interest is negligible, the mode functions $\mathbf{U}_\mu$ satisfy the relation $\int_{-\infty}^{\infty}dx\, n^2(x)\mathbf{U}_{\omega\mathbf{K}qj}^{*}(x)\mathbf{U}_{\omega'\mathbf{K}q'j'}(x) = 2\pi c^2(\beta_j/\omega)\delta(\omega-\omega')\delta_{qq'}\times\delta_{jj'}$. Here, $n(x)=n_1$ for $x<0$ and $n(x)=n_2$ for $x>0$. Hence, we can show that the energy of the field is $\epsilon_0\int d\mathbf{r}\, n^2(x)|\mathbf{E}(\mathbf{r})|^2=\Sigma_\mu(a_\mu^{\dagger}a_\mu+a_\mu a_\mu^{\dagger})/2$. Here, $\int d\mathbf{r}=\int_{-\infty}^{\infty}dx\int_{-\infty}^{\infty}dy\int_{-\infty}^{\infty}dz$ is the integral over the whole space.

We now present the Hamiltonian for the atom-field interaction. In the dipole and rotating-wave approximations and in the interaction picture, the atom-field interaction Hamiltonian is

$$H_{\text{int}} = -i\hbar\sum_{\mu ab}G_{\mu ab}\sigma_{ab}a_{\mu}e^{-i(\omega-\omega_{ab})t} + \text{H.c.} \quad (7)$$

Here, $\sigma_{ab}=|a\rangle\langle b|$ describes the atomic transition from the level b to the level a, $\omega_{ab}=\omega_a-\omega_b$ is the angular frequency of the transition, and

$$G_{\mu ab} = \frac{k}{4\pi\sqrt{\pi\epsilon_0\hbar\beta_j}}e^{i\mathbf{K}\cdot\mathbf{R}}\langle\varphi_a|\mathbf{U}_{\mu}\cdot\mathbf{d}_{eg}|\varphi_b\rangle \quad (8)$$

is the coupling coefficient. In expression (8), $\mathbf{d}_{eg}$ is the dipole moment of the atom and $\mathbf{R}=(y,z)$ is the projection of the position vector $\mathbf{r}=(x,y,z)$ of the atom onto the interface plane.

III. BASIC EQUATIONS FOR SPONTANEOUS RADIATIVE DECAY OF THE ATOM

We use the mode expansion approach and the Weisskopf-Wigner formalism [35] to derive the microscopic dynamical equations for spontaneous radiative decay of the atom in the surfaced-induced potential. For convenience, we introduce the notation $\sigma_{\nu\nu'}=|\nu\rangle\langle\nu'|$ and $\omega_{\nu\nu'}=\omega_\nu-\omega_{\nu'}$ for the transition operator and the transition frequency, respectively, of an arbitrary pair of levels ν and ν'. We first study the time evolution of an arbitrary atomic operator $\mathcal{O}$. The Heisenberg equation for this operator is

$$\dot{\mathcal{O}} = \sum_{\mu ab}(G_{\mu ab}[\sigma_{ab},\mathcal{O}]a_{\mu}e^{-i(\omega-\omega_{ab})t} + G_{\mu ab}^{*}a_{\mu}^{\dagger}[\mathcal{O},\sigma_{ba}]e^{i(\omega-\omega_{ab})t}). \quad (9)$$

Meanwhile, the Heisenberg equation for the photon operator a_μ is $\dot{a}_\mu=\Sigma_{ab}G_{\mu ab}^{*}\sigma_{ba}e^{i(\omega-\omega_{ab})t}$. Integrating this equation, we find

$$a_{\mu}(t) = a_{\mu}(t_0) + \sum_{ab}G_{\mu ab}^{*}\int_{t_0}^{t}dt'\sigma_{ba}(t')e^{i(\omega-\omega_{ab})t'}. \quad (10)$$

We consider the situation where the field is initially in the vacuum state. We assume that the evolution time $t-t_0$ and the characteristic atomic lifetime τ are large as compared to the characteristic optical period T. Under these conditions, since the continuum of the field modes is broadband, the Markov approximation $\sigma_{ba}(t')=\sigma_{ba}(t)$ can be applied to describe the back action of the second term in Eq. (10) on the atom [35]. Under the condition $t-t_0\gg T$, we calculate the integral with respect to t' in the limit $t-t_0\to\infty$. We set aside the imaginary part of the integral, which describes the frequency shift. Such a shift is usually small. We can effectively account for it by incorporating it into the atomic frequency and the surface-atom potential. With the above approximations, we obtain

$$a_{\mu}(t) = a_{\mu}(t_0) + \pi\sum_{ab}G_{\mu ab}^{*}\sigma_{ba}(t)\delta(\omega-\omega_{ab}). \quad (11)$$

Inserting Eq. (11) into Eq. (9) yields the Heisenberg-Langevin equation

$$\dot{\mathcal{O}} = \frac{1}{2}\sum_{aa'bb'}(\gamma_{aa'bb'}[\sigma_{a'b'},\mathcal{O}]\sigma_{ba}e^{-i(\omega_{ab}-\omega_{a'b'})t} + \gamma_{aa'bb'}^{*}\sigma_{ab}[\mathcal{O},\sigma_{b'a'}]e^{i(\omega_{ab}-\omega_{a'b'})t}) + \xi_{\mathcal{O}}. \quad (12)$$

Here,

$$\gamma_{aa'bb'} = 2\pi\sum_{\mu}G_{\mu ab}^{*}G_{\mu a'b'}\delta(\omega-\omega_{ab}) \quad (13)$$

are the decay coefficients and $\xi_{\mathcal{O}}$ is the noise operator. We emphasize that Eq. (12) can be applied to any atomic operators.

We now examine the time evolution of the reduced density operator ρ of the atomic system. We multiply Eq. (12) by $\rho(0)$, take the trace of the result, use the relation $\text{Tr}[\mathcal{O}(t)\rho(0)]=\text{Tr}[\mathcal{O}(0)\rho(t)]$, transform to arrange the opera-

tor $\mathcal{O}(0)$ at the first position in each operator product, and eliminate $\mathcal{O}(0)$. Then, we obtain the Liouville equation

$$\dot{\rho} = \frac{1}{2}\sum_{aa'bb'} [\gamma_{aa'bb'}(\sigma_{ba}\rho\sigma_{a'b'} - \delta_{bb'}\sigma_{a'a}\rho)e^{-i(\omega_{ab}-\omega_{a'b'})t} + \gamma^{*}_{aa'bb'}(\sigma_{b'a'}\rho\sigma_{ab} - \delta_{bb'}\rho\sigma_{aa'})e^{i(\omega_{ab}-\omega_{a'b'})t}]. \quad (14)$$

For the matrix elements $\rho_{\nu\nu'}=\langle\nu|\rho|\nu'\rangle$, the above equations yields

$$\dot{\rho}_{aa'} = -\frac{1}{2}\sum_{a''}(\gamma_{a''a}e^{i\omega_{aa''}t}\rho_{a''a'} + \gamma^{*}_{a''a'}e^{i\omega_{a''a'}t}\rho_{aa''}),$$

$$\dot{\rho}_{ab} = -\frac{1}{2}\sum_{a'}\gamma_{a'a}e^{i\omega_{aa'}t}\rho_{a'b},$$

$$\dot{\rho}_{bb'} = \frac{1}{2}\sum_{aa'}(\gamma_{aa'bb'} + \gamma^{*}_{a'ab'b})e^{i(\omega_{bb'}-\omega_{aa'})t}\rho_{aa'}, \quad (15)$$

where $\gamma_{aa'}=\Sigma_b\gamma_{aa'bb}=2\pi\Sigma_{\mu b}G^{*}_{\mu ab}G_{\mu a'b}\delta(\omega-\omega_{ab})$. Equations (15) show that the spontaneous decay rate for a transition $a\rightarrow b$ is given by $\gamma_{ab}=\gamma_{aabb}=2\pi\Sigma_{\mu}|G_{\mu ab}|^2\delta(\omega-\omega_{ab})$. Meanwhile, the total decay rate for an excited level a is $\gamma_a=\gamma_{aa}=2\pi\Sigma_{\mu b}|G_{\mu ab}|^2\delta(\omega-\omega_{ab})$. It is obvious that $\gamma_a=\Sigma_b\gamma_{ab}$.

Equations (15) correspond to the incoherent radiative decay part of the master equation for an atom interacting with external fields in the proximity of a surface. A set of more general equations is presented in Appendix B for the case where the atom is driven by classical coherent plane-wave fields. We note that the terms in Eqs. (15) are different from and much more complicated than the conventional phenomenological decay terms [36]. The unusual structure of Eqs. (15) results from the complexity of the translational levels of the atom in the surface-induced potential. Similar structures are also observed in the case of a multilevel alkali-metal atom [4,37].

It is worth noting that the inclusion of the imaginary part of the integral in Eq. (10) would lead to the dependence of the surface-atom potential on the transition between translational levels. The study of such frequency shifts is beyond the scope of the present paper.

We emphasize that the results of this section do not depend on the specific form of the confining potential. Therefore, these results can, in principle, be extended to describe the radiative decay of vibrational levels of a molecule.

IV. SPONTANEOUS RADIATIVE DECAY RATES

In the half-space $x>0$, where the atom is restricted to, the mode functions of the radiation field are described by expressions (5). We insert these expressions into Eq. (8) and then the result into Eq. (13). We perform the summation with respect to the mode index μ. Then, in the case where the dipole moment $\mathbf{d}_{eg}$ is perpendicular to the interface, we obtain

$$\gamma^{\perp}_{aa'bb'} = \frac{3}{2}\gamma_f(\omega_{ab})\left\{\int_0^1 \mathrm{Re}[(1-\xi^2)F_{ab}(\xi k_{ab})F^{*}_{a'b'}(\xi k_{ab}) + r_{\perp}(\xi)F_{ab}(\xi k_{ab})F_{a'b'}(\xi k_{ab})]d\xi + \int_0^{\sqrt{n_1^2-1}} T_{\perp}(\xi)I_{ab}(\xi k_{ab})I_{a'b'}(\xi k_{ab})d\xi\right\}, \quad (16)$$

and, in the case where the dipole moment $\mathbf{d}_{eg}$ is parallel to the interface, we find

$$\gamma^{\parallel}_{aa'bb'} = \frac{3}{4}\gamma_f(\omega_{ab})\left\{\int_0^1 \mathrm{Re}[(1+\xi^2)F_{ab}(\xi k_{ab})F^{*}_{a'b'}(\xi k_{ab}) + r_{\parallel}(\xi)F_{ab}(\xi k_{ab})F_{a'b'}(\xi k_{ab})]d\xi + \int_0^{\sqrt{n_1^2-1}} T_{\parallel}(\xi)I_{ab}(\xi k_{ab})I_{a'b'}(\xi k_{ab})d\xi\right\}. \quad (17)$$

Here we have introduced the notation

$$r_{\perp}(\xi) = (1-\xi^2)\frac{n_1^2\xi - \sqrt{n_1^2-1+\xi^2}}{n_1^2\xi + \sqrt{n_1^2-1+\xi^2}},$$

$$r_{\parallel}(\xi) = \frac{\xi - \sqrt{n_1^2-1+\xi^2}}{\xi + \sqrt{n_1^2-1+\xi^2}} - \xi^2\frac{n_1^2\xi - \sqrt{n_1^2-1+\xi^2}}{n_1^2\xi + \sqrt{n_1^2-1+\xi^2}} \quad (18)$$

and

$$T_{\perp}(\xi) = \frac{2n_1^2}{n_1^2-1}\frac{\sqrt{n_1^2-1-\xi^2}}{(n_1^2+1)\xi^2+1}\xi(1+\xi^2),$$

$$T_{\parallel}(\xi) = \frac{2}{n_1^2-1}\left(1+\frac{n_1^2\xi^2}{(n_1^2+1)\xi^2+1}\right)\xi\sqrt{n_1^2-1-\xi^2}. \quad (19)$$

The quantity

$$\gamma_f(\omega) = \frac{d_{eg}^2\omega^3}{3\pi\epsilon_0\hbar c^3} \quad (20)$$

is the natural linewidth of a two-level atom with the transition frequency ω and the dipole moment d_{eg}. The matrix elements

$$F_{ab}(\beta) = \langle\varphi_a|e^{i\beta x}|\varphi_b\rangle,$$

$$I_{ab}(\beta) = \langle\varphi_a|e^{-\beta x}|\varphi_b\rangle \quad (21)$$

for the transitions between the translational eigenstates $|\varphi_a\rangle$ and $|\varphi_b\rangle$ have been introduced. In deriving Eqs. (16) and (17) we have changed the integration variable K to $\xi=\sqrt{|1-\kappa^2|}$. Here the parameter $\kappa=K/k_{ab}$ with $k_{ab}=\omega_{ab}/c$ has been introduced.

The functions $r_{\perp}$ and $r_{\parallel}$ are related to the reflection coefficients $r_{21}^{s}=(\xi-\eta)/(\xi+\eta)$ and $r_{21}^{p}=(n_1^2\xi-\eta)/(n_1^2\xi+\eta)$ as given by $r_{\perp}=\kappa^2 r_{21}^{p}$ and $r_{\parallel}=r_{21}^{s}-\xi^2 r_{21}^{p}$. Here, $\kappa=\sqrt{1-\xi^2}$ and $\eta=\sqrt{n_1^2-1+\xi^2}$. Hence, the terms that contain $r_{\perp}$ and $r_{\parallel}$ in Eqs. (16) and (17) are the results of the interference between the emitted and reflected fields. Meanwhile, the functions $T_{\perp}$ and $T_{\parallel}$ are related to the transmission coefficients t_{12}^{s}

$=2\eta/(\eta+i\xi)$ and $t_{12}^{p}=2n_1\eta/(\eta+in_1^2\xi)$ of the evanescent modes as given by $T_{\perp}=(\xi/2\eta)\kappa^2|t_{12}^{p}|^2$ and $T_{\parallel}=(\xi/2\eta)(|t_{12}^{s}|^2+\xi^2|t_{12}^{p}|^2)$. Here, $\kappa=\sqrt{1+\xi^2}$ and $\eta=\sqrt{n_1^2-1-\xi^2}$. Hence, the terms that contain $T_{\perp}$ and $T_{\parallel}$ in Eqs. (16) and (17) are the results of emission into the evanescent modes.

According to Eqs. (21), the factors $F_{ab}(\beta)$ and $I_{ab}(\beta)$ are determined by the overlap and interference between the translational wave functions φ_a and φ_b. Such an overlap and interference can be physically interpreted as the overlap and interference between the de Broglie waves of the atom. The factors $|F_{ab}(0)|^2$ and $|I_{ab}(0)|^2$, with the argument $\beta=0$, are equal to each other and coincide with the Franck-Condon factors $|\langle\varphi_a|\varphi_b\rangle|^2$. The exponential factors $e^{i\beta x}$ and $e^{-\beta x}$ in Eqs. (21) take into account the momentum of the photon emitted or absorbed by the atom (see Appendix B). The factor $e^{i\beta x}$ corresponds to the case where the mode is a propagating mode, and the factor $e^{-\beta x}$ corresponds to the case where the mode is an evanescent mode. Thus, $F_{ab}(\beta)$ characterizes the strength of the translational transition with the participation of a propagating-mode photon, and $I_{ab}(\beta)$ corresponds to the case of an evanescent-mode photon.

We assume that the orientation of the atomic dipole moment is completely random. In this case, the averaged decay parameters are given by $\gamma_{aa'bb'}=(\gamma^{\perp}_{aa'bb'}+2\gamma^{\parallel}_{aa'bb'})/3$. Using Eqs. (16) and (17), we find

$$\gamma_{aa'bb'}=\gamma_f(\omega_{ab})\left\{\int_0^1 \mathrm{Re}\left(F_{ab}(\xi k_{ab})F^{*}_{a'b'}(\xi k_{ab})+\frac{r_{\perp}(\xi)+r_{\parallel}(\xi)}{2}F_{ab}(\xi k_{ab})F_{a'b'}(\xi k_{ab})\right)d\xi+\int_0^{\sqrt{n_1^2-1}}\frac{T_{\perp}(\xi)+T_{\parallel}(\xi)}{2}I_{ab}(\xi k_{ab})I_{a'b'}(\xi k_{ab})d\xi\right\}. \tag{22}$$

We note that all the decay coefficients are real quantities.

When we set $a'=a$ and $b'=b$ in Eq. (22), we obtain the following expression for the spontaneous transition rate:

$$\gamma_{ab}=\gamma_f(\omega_{ab})\left\{\int_0^1\left(|F_{ab}(\xi k_{ab})|^2+\frac{r_{\perp}(\xi)+r_{\parallel}(\xi)}{2}\mathrm{Re}[F_{ab}^2(\xi k_{ab})]\right)d\xi+\int_0^{\sqrt{n_1^2-1}}\frac{T_{\perp}(\xi)+T_{\parallel}(\xi)}{2}I_{ab}^2(\xi k_{ab})d\xi\right\}. \tag{23}$$

Equation (23) shows that the effects of the dielectric on the spontaneous transition rate γ_{ab} appear through (a) the shift of the transition frequency ω_{ab}, (b) the overlap and interference between the center-of-mass wave functions, (c) the interference between the emitted and reflected fields, and (d) the transmission into the evanescent modes.

The cross decay coefficient $\gamma_{aa'}=\Sigma_b\gamma_{aa'bb}$ is the sum of $\gamma_{aa'bb}$ over the ground-state levels b. The summation can be simplified if, for each fixed index a, the overlapping factors F_{ab} and I_{ab} are substantial only in a small region of b. In this case, the transition frequency ω_{ab} in expression (22) can be replaced by an effective frequency $\omega_{a\bar{b}}$ that does not depend on b. We use this approximation, set $b'=b$, and sum up the result with respect to b. Then, with the help of the relation $\Sigma_b|\varphi_b\rangle\langle\varphi_b|=1$, we obtain

$$\gamma_{aa'}=\langle\varphi_a|\gamma_x(\omega_{a\bar{b}})|\varphi_{a'}\rangle. \tag{24}$$

Here,

$$\gamma_x(\omega)=\gamma_f(\omega)\left\{1+\int_0^1\frac{r_{\perp}(\xi)+r_{\parallel}(\xi)}{2}\cos(2\xi kx)d\xi+\int_0^{\sqrt{n_1^2-1}}\frac{T_{\perp}(\xi)+T_{\parallel}(\xi)}{2}e^{-2\xi kx}d\xi\right\} \tag{25}$$

is the spontaneous emission rate of a two-level atom with frequency ω, being at rest in the vicinity of the dielectric [16,17]. In order to find the linewidth γ_a, we set $a=a'$ in Eq. (24). Then, we obtain

$$\gamma_a=\langle\varphi_a|\gamma_x(\omega_{a\bar{b}})|\varphi_a\rangle. \tag{26}$$

The above equation means that the radiative linewidth γ_a can be approximately considered as the average of the atom-at-rest decay rate $\gamma_x(\omega_{a\bar{b}})$ with respect to the center-of-mass wave function $\varphi_a(x)$.

We note that, in the case where the refractive index n_1 of the dielectric is not large, the reflection of light from the interface and the emission of light into the evanescent modes are not strong. In this case, $\gamma_x(\omega)$ with a fixed argument ω is a slowly varying function of x. Hence, for $a\neq a'$, since $|a\rangle$ and $|a'\rangle$ are orthogonal to each other, the quantity $\gamma_{aa'}$ is usually small compared to γ_a and $\gamma_{a'}$.

We emphasize that the first integral in Eq. (25) results from the interference between the emitted and reflected fields. The second integral in Eq. (25) results from the emission into the evanescent modes. We note that expression (25) for γ_x is in full agreement with the results of the linear-response formalism [16,17]. However, the results of Refs. [16,17] are written in a different form that is difficult to identify the origins and physical meanings of the contributions.

If we neglect reflection from the interface and emission into the evanescent modes and limit ourselves to considering only levels with negligible surfaced-induced frequency shifts, then Eq. (22) reduces to

$$\gamma_{aa'bb'}=\gamma_0 f_{aa'bb'}, \tag{27}$$

where $\gamma_0=\gamma_f(\omega_0)$, $\omega_0=\omega_e-\omega_g$, and

$$f_{aa'bb'}=\frac{1}{2}\int_{-1}^{1}d\xi\langle\varphi_a|e^{i\xi k_0 x}|\varphi_b\rangle\langle\varphi_{b'}|e^{-i\xi k_0 x}|\varphi_{a'}\rangle=\int_{-\infty}^{\infty}\int_{-\infty}^{\infty}dxdx'\frac{\sin k_0(x-x')}{k_0(x-x')}\times\varphi_a(x)\varphi_b(x)\varphi_{a'}(x')\varphi_{b'}(x'). \tag{28}$$

Setting $b'=b$ in expressions (27) and (28) and summing up

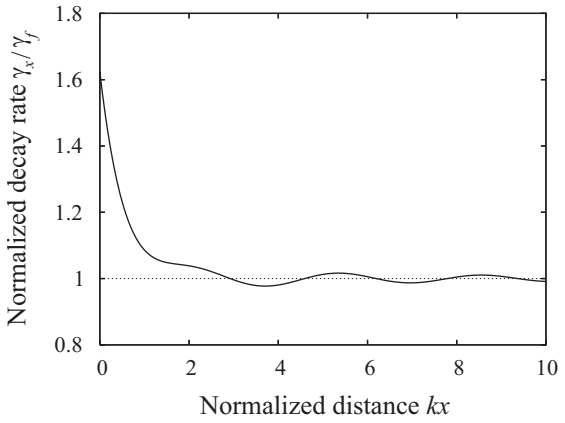

FIG. 6. Normalized decay rate $\gamma_x(\omega)/\gamma_f(\omega)$ of a two-level atom rested at a point in the vicinity of a semi-infinite dielectric medium as a function of the normalized surface-atom distance kx. The refractive index of the medium is $n_1=1.45$.

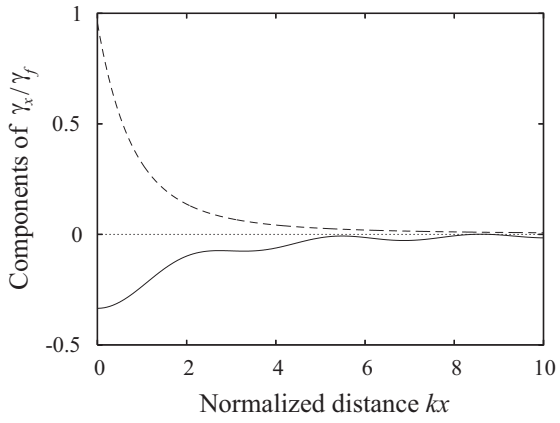

FIG. 7. Contributions of the first (solid line) and second (dashed line) integrals in Eq. (25) to the normalized decay rate $\gamma_x(\omega)/\gamma_f(\omega)$ of Fig. 6.

the resultant expressions over b, we find $\gamma_{aa'}=\gamma_0\langle a|a'\rangle = \gamma_0\delta_{aa'}$.

V. NUMERICAL RESULTS

In what follows, we present the results of our numerical calculations for the spontaneous radiative decay characteristics of the atom. As stated in Sec. II, we use the parameters of fused silica, for the dielectric, and the parameters of atomic cesium with the D_2 line, for the atom. The parameters are given in Sec. II.

We first consider the case where the atom is at rest [14,16,17]. We plot in Fig. 6 the normalized decay rate $\gamma_x(\omega)/\gamma_f(\omega)$ as a function of the normalized surface-atom distance kx. The figure shows that $\gamma_x(\omega)/\gamma_f(\omega)$ varies slowly with kx. We observe not only enhancement, $\gamma_x/\gamma_f>1$, but also inhibition, $\gamma_x/\gamma_f<1$, of spontaneous emission, depending on the position of the atom. As pointed in Refs. [14,16,17], such changes are quantum electrodynamic effects resulting from modifications of the field modes in the presence of the dielectric. The maximum value of $\gamma_x(\omega)/\gamma_f(\omega)$ is about 1.6, achieved at $kx=0$. Such a quantum enhancement is moderate. It is not dramatic. The reason is that the refractive index of silica, $n_1=1.45$, is not large. We observe small oscillations in $\gamma_x(\omega)/\gamma_f(\omega)$ as kx increases. Such oscillations are due to the interference between the emitted and reflected fields.

The deviation of $\gamma_x(\omega)/\gamma_f(\omega)$ from unity is caused by the interference between the emitted and reflected fields and by the emission into the evanescent modes, which are expressed by the first and second integrals in Eq. (25), respectively. We calculate these integrals separately and plot the results in Fig. 7. The solid curve of the figure shows that, for $kx\leqslant 8$, the first integral is negative. Thus, in the close vicinity of the interface, the interference between the emitted and reflected fields is destructive and hence tends to reduce the spontaneous decay rate. The solid curve of the figure also shows that, in the region of large kx, the first integral can become positive—that is, the interference can be constructive—depending on the position of the atom. Meanwhile, the dashed curve of the figure shows that the second integral in Eq. (25) is always positive. Thus, the emission into the evanescent modes always enhances the spontaneous decay rate. Such an enhancement is due to the existence and confinement of the evanescent modes.

Due to the surface-atom potentials V_e and V_g, the transition frequency of the atom varies in space as given by $\omega=\omega_x=\omega_0+[V_e(x)-V_g(x)]/\hbar$. Consequently, when we take into account the frequency shift, the decay rate of the atom is $\gamma_x(\omega_x)$. The spatial dependence of $\gamma_x(\omega_x)$ is determined not only by the change in the mode structure but also by the change in the atomic transition frequency ω_x. We plot the spatial dependence of $\gamma_x(\omega_x)$ in Fig. 8. The figure and the inset show that, when x decreases from 1 nm to 0.2 nm, the decay rate drops quickly from its peak value. The reason is that, in this region of space, the surface-induced frequency shift of the transition is negative (redshift) and substantial.

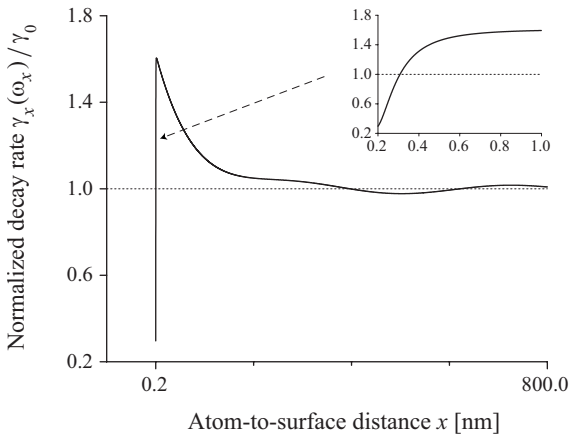

FIG. 8. Normalized decay rate $\gamma_x(\omega_x)/\gamma_0$ of a two-level atom with a space-dependent frequency, rested at a point in the vicinity of a semi-infinite medium. The transition frequency ω_x is shifted from the free-space transition frequency ω_0 by the surface-atom interaction. The parameters of the potentials are as in Fig. 1. The refractive index of the medium is $n_1=1.45$. The wavelength of the transition of the atom in free space is $\lambda_0=852$ nm.

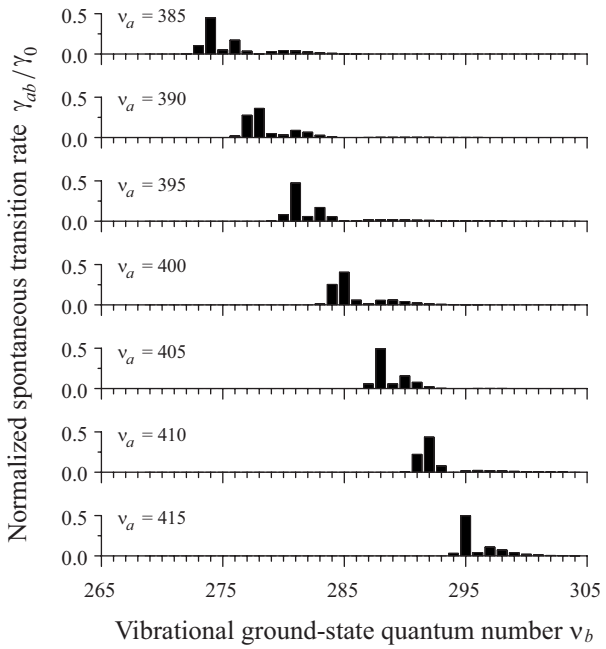

FIG. 9. Spontaneous transition rates γ_{ab} for levels with large vibrational quantum numbers. The rates are normalized to the free-space spontaneous decay rate γ_0. The parameters used are as in Figs. 1, 2, and 8.

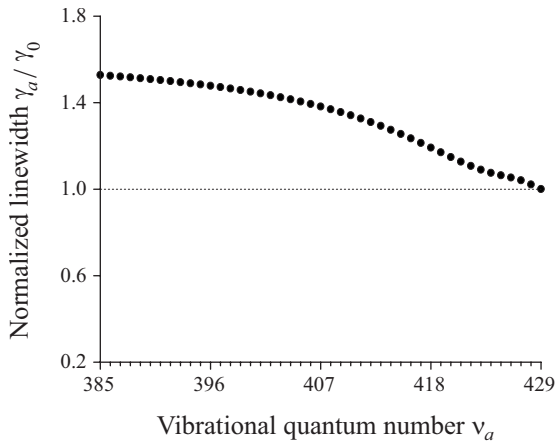

FIG. 10. Radiative linewidths γ_a of bound excited-state levels with large vibrational quantum numbers. The linewidths are normalized to the free-space spontaneous decay rate γ_0. The parameters used are as in Figs. 1, 2, and 8.

Such a shift of ω_x reduces the natural linewidth $\gamma_f(\omega_x)$ [see Eq. (20)] and hence reduces the decay rate $\gamma_x(\omega_x)$ [see Eq. (25)]. The effects of the transition frequency shift and the quantum enhancement on the decay are substantial in the regions $x \lesssim [(C_{3e}-C_{3g})/\hbar\omega_0]^{1/3}=0.16$ nm and $x \lesssim \lambda_0 = 852$ nm, respectively. The two scales are quite different from each other: $[(C_{3e}-C_{3g})/\hbar\omega_0]^{1/3} \ll \lambda_0$. In the region $x > 1$ nm, the frequency shift of the transition is small and hence the spatial dependence of the decay rate is mainly determined by the mode structure of the field. Meanwhile, in the region from 1 nm to 0.2 nm, the effect of the frequency shift is dominant. We note that, in the region $x < 0.2$ nm, which is not shown in the figure, the transition frequency shift may become positive, leading to an enhancement of the decay rate $\gamma_x(\omega_x)$. In this region, the potential slope is steep, the force is large, and consequently consideration of the center-of-mass motion of the atom must be included. Due to the lack of quantitative information about the silica-cesium repulsive potential and due to the need to include the center-of-mass motion of the atom, we do not plot the decay rate $\gamma_x(\omega_x)$ in the region $x < 0.2$ nm. The cutoff value of 0.2 nm is chosen because it is close to the position $x_m=0.19$ nm of the minima of the potentials V_e and V_g.

In the close vicinity of the surface, the atom cannot be at rest because of the force resulting from the gradient of the surface-induced potential. In this region, we must take into account the center-of-mass motion of the atom. To do this in a fully quantum treatment, we must consider the sets of combined states $\{|a\rangle\}$ and $\{|b\rangle\}$ instead of the internal states $|e\rangle$ and $|g\rangle$. We plot in Fig. 9 the spontaneous transition rate γ_{ab} for various pairs of shallow levels a and b, which have large vibrational quantum numbers. The figure shows that each upper level a can be substantially coupled to a number of lower levels b in a finite interval of ν_b. The boundary values of this interval tend to become larger when ν_a increases. In general, γ_{ab} varies unevenly with increasing ν_a or ν_b. Such features are due to the fact that the rate γ_{ab} substantially depends on the factors F_{ab} and I_{ab} [see Eq. (23)], which describe the overlap and interference between the de Broglie waves of the atomic center-of-mass states φ_a and φ_b [see Eqs. (21)]. When the overlap is large and the interference is constructive, the factors F_{ab} and I_{ab} are substantial. In this case, the transition rate γ_{ab} is large. When the overlap is small or the interference is destructive, the factors F_{ab} and I_{ab} are small. In this case, the transition rate γ_{ab} is small. The interval of ν_b that can be coupled to a given ν_a is determined by the condition for the spatial overlap between the de Broglie waves. The modulations in magnitude of γ_{ab} in this interval are caused by the effect of the interference between the de Broglie waves. Note that, in the case of shallow bound levels, the transition frequency shift $\omega_{ab}-\omega_0$ is small compared to the free-space optical frequency ω_0 (see Fig. 3). In this case, the effect of the frequency shift on the spontaneous transition rate is negligible.

We use the approximate equation (26) to calculate the linewidths γ_a of shallow bound excited-state levels a, with large quantum numbers ν_a, in the range from 385 to 429, and plot the results in Fig. 10. The figure shows that γ_a/γ_0 increases slowly from 1 to 1.53 as ν_a reduces from 429 to 385. The observed enhancement of γ_a is the average of the quantum enhancement of the atom-at-rest decay rate $\gamma_x(\omega_{a\bar{b}})$ with respect to the center-of-mass wave function $\varphi_a(x)$ [see Eq. (26)]. When ν_a is large enough, the surface-induced transition frequency shift is small, i.e., $\omega_{a\bar{b}} \cong \omega_0$. In this case, the magnitude of γ_a is mainly determined by the mode structure. When ν_a is not too large, the center-of-mass wave function $\varphi_a(x)$ is confined to a small spatial region close to the surface and, hence, quantum enhancement of γ_a is observed. The spatial spread of $\varphi_a(x)$ increases with increasing ν_a. This explains why γ_a reduces with increasing ν_a in Fig. 10. When ν_a is very large, the quantum enhancement is negligible and, hence, we have $\gamma_a \cong \gamma_0$.

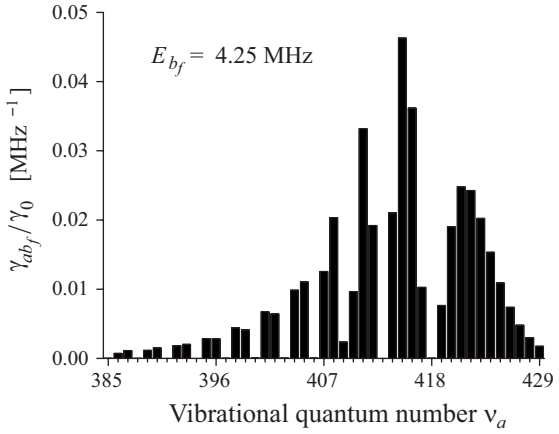

FIG. 11. Normalized density γ_{ab_f}/γ_0 for the rate of spontaneous radiative decay from a bound excited-state level a to a free ground-state level b_f as a function of the vibrational quantum number ν_a. The parameters used are as in Figs. 1, 2, and 8.

The spectra of translational levels of ground and excited states include not only bound levels but also free levels. Both types of levels can be coupled to each other. Since the center-of-mass wave functions of free excited-state levels a_f and free ground-state levels b_f are normalized per unit energy, the quantities γ_{ab_f}, γ_{a_fb}, and $\gamma_{a_fb_f}$ are the densities of the spontaneous decay rates for the transitions $a \to b_f$, $a_f \to b$, and $a_f \to b_f$, respectively. Knowledge of these quantities is required for the study of the dynamical and spectroscopic characteristics of moving atoms. In this connection, we plot in Fig. 11 the normalized density γ_{ab_f}/γ_0 for the rate of spontaneous decay from a bound excited-state level a to a free ground-state level b_f as a function of the vibrational quantum number ν_a. Figure 11 shows irregular modulations in the dependence of γ_{ab_f} on ν_a. Similar to the case of Fig. 9,

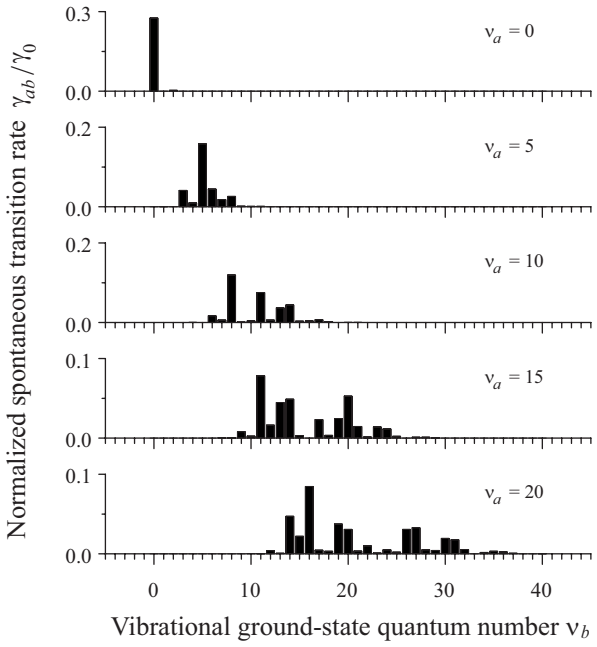

FIG. 12. Same as Fig. 8 but for levels with small vibrational quantum numbers.

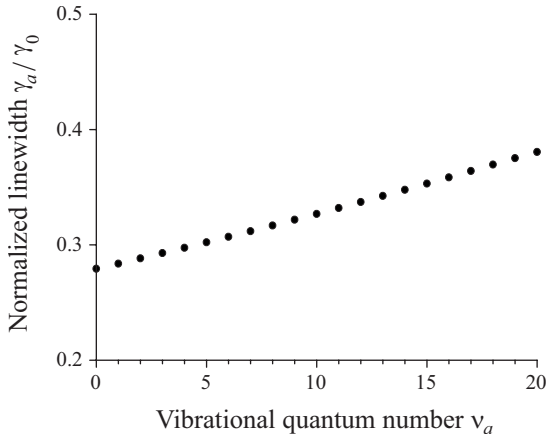

FIG. 13. Same as Fig. 10 but for levels with small vibrational quantum numbers.

such modulations are caused by the effect of the interference between the excited- and ground-state atomic de Broglie waves. Due to the destructive interference, the factors F_{ab_f} and I_{ab_f} and, consequently, the transition rate density γ_{ab_f} can become almost negligible for some specific values of ν_a.

The effect of the surface-induced shifts of the transition frequencies on the transition rates and linewidths becomes substantial when the translational eigenfunctions of the atom are close to the surface—that is, when the levels are deep. We plot in Figs. 12 and 13 the spontaneous transition rates γ_{ab} and the linewidths γ_a, respectively, for deep bound levels, with small vibrational quantum numbers. Our additional numerical calculations (not presented here) show that the transitions from bound excited-state levels with small ν_a to free ground-state levels are negligible. Due to this fact, the sum of the values of the individual transition rates γ_{ab} presented in each fixed row of Fig. 12 almost coincides with the corresponding value of the linewidth γ_a in Fig. 13. Figure 13 shows that, for small ν_a, the surface-modified linewidth γ_a is smaller than the free-space linewidth γ_0, and γ_a reduces with decreasing ν_a. Such a reduction of the radiative linewidth γ_a is caused by the surface-induced redshifts of the significant-component transition frequencies $\omega_{ab'}$. Indeed, $\omega_{ab'}$ reduces with decreasing ν_a and becomes substantially smaller than ω_0 when the level a is deep enough. This decrease of $\omega_{ab'}$ leads to a reduction of $\gamma_f(\omega_{ab'})$ [see Eq. (20)] through a decrease of the mode density [35]. When such a reduction is substantial enough, it may result in a reduction of $\gamma_{ab'}$ [see Eq. (23)]. This in turn leads to a reduction of γ_a. We note that the minimum value of the radiative linewidth γ_a is observed for $\nu_a=0$ and is about $0.28\gamma_0$. This value is substantially (about 3.6 times) smaller than the natural linewidth γ_0 of the atom. We note that, when the atomic center-of-mass states are close to the surface and the surface temperature is high, the decay of the atom due to the interaction with the phonons of the solid may become important [3]. However, the study of the decay due to phonons is beyond the scope of this paper.

VI. CONCLUSIONS

We have studied spontaneous radiative decay of translational levels of an atom in the vicinity of a semi-infinite

dielectric. We have systematically derived the microscopic dynamical equations for the spontaneous decay process. Our general formalism is applicable, in principle, to any confining potential. We have calculated analytically and numerically the spontaneous transition rates between the translational excited and ground states and the radiative linewidths of the bound excited states. We have shown that the effects of the dielectric on the spontaneous transition rates and radiative linewidths appear through (a) the shift of the transition frequency, (b) the overlap and interference between the center-of-mass wave functions, (c) the interference between the emitted and reflected fields, and (d) the transmission into the evanescent modes. Our numerical calculations for the silica-cesium interaction have demonstrated that the radiative linewidths of the bound excited levels with large enough but not too large vibrational quantum numbers are moderately enhanced by the emission into the evanescent modes and those for the deep bound levels are substantially reduced by the surface-induced redshift of the transition frequency. In the numerical calculations, because of the complexity of surface physics and the lack of data, we were forced to use a specific potential model whose parameters may be different from the actual ones. However, we believe that the quantitative differences are not dramatic and, therefore, the qualitative aspects are correctly reflected, at least for shallow bound and free states, in which the atom spends most of its time far away from the interface. We also recognize that our model does not take into account the effect of surface-induced level crossing, which may occur at small atom-surface distances, with the participation of high-lying internal levels. Because of various limitations, our model is not adequate for very small atom-surface distances. Nevertheless, our approach can be extended and our results can provide an impetus for scientific debate.

ACKNOWLEDGMENTS

We thank M. Oriá, S. Dutta Gupta, and P. N. Melentiev for fruitful discussions. This work was carried out under the 21st Century COE program on "Coherent Optical Science."

APPENDIX A: PARAMETERS OF THE SILICA-CESIUM POTENTIAL

The actual form of the surface-atom potential is unknown [22]. For the purpose of numerical demonstration of our formalism, we choose the model $V(x)=Ae^{-\alpha x}-C_3/x^3$ [2,22]. Under the condition $\alpha^3 C_3/A<256/3e^4$, this potential has a peak at $x_p=\xi_p/\alpha$ and a local minimum at $x_m=\xi_m/\alpha$, where $\xi_p<4$ and $\xi_m>4$ are solutions to the equation $\xi^4 e^{-\xi}=3\alpha^3 C_3/A$. The peak value $V(x_p)$ should be positive and large enough to create a steep slope for the potential $V(x)$ in the small interval (x_p,x_m). Such a slope leads to a substantial repulsive force on the atom in the close vicinity of the surface. We discard the region $x<x_p$, assuming that the atom is outside and cannot penetrate into this region of space.

The depth of the potential is defined by $D=-V(x_m)=-Ae^{-\alpha x_m}+C_3/x_m^3$. We find the relation

$$A=\frac{3D}{\alpha x_m-3}e^{\alpha x_m}. \tag{A1}$$

In terms of the parameter $x_a=\sqrt[3]{C_3/D}$, we have

$$\alpha=\frac{3}{x_m[1-(x_m/x_a)^3]}. \tag{A2}$$

Equations (A1) and (A2) allow us to determine the parameters A and α from the parameters C_3, D, and x_m. Since $\alpha>0$ and $\alpha x_m>4$, the condition

$$\frac{x_a}{\sqrt[3]{4}}<x_m<x_a \tag{A3}$$

must be satisfied.

Many parameters of the silica-cesium potential are yet to be ascertained [2,3,22,23]. We list a few available theoretical and experimental data and speculate about the other parameters. According to Ref. [23], the van der Waals coefficient for the interaction between a ground-state cesium atom and a perfect metal surface is $C_3^{(\mathrm{metal})}=4.5$ a.u.$=4.39$ kHz μm^3. For a dielectric medium of refractive index n, we have an approximate expression $C_3=(n^2-1)/(n^2+1)C_3^{(\mathrm{metal})}$ [22]. For pure fused silica, with $n=1.45$ (in a broad region around the wavelength $\lambda_0=852$ nm), we find $C_{3g}=1.56$ kHz μm^3. This theoretical value is larger than the theoretical estimate of Ref. [24], which ignores core transitions. Since the van der Waals coefficient C_{3e} for the cesium excited state $6P_{3/2}$ has not been accurately calculated in the manner of Ref. [23], we take a relatively arbitrary value $C_{3e}=3.09$ kHz μm^3. This choice is based on the fact that, from the results of Ref. [24] (see also [25]), where the core contributions are neglected, one can infer the ratio $C_{3e}/C_{3g}=1.98$. Regarding the potential depths, we use the experimental value $D_g=0.66$ eV $=159.6$ THz, measured as the adsorption energy of ground-state cesium atoms on fused silica [26]. With the assumption $D_e/D_g=C_e/C_g$, we find $D_e=316$ THz. For both the ground- and excited-state potentials, we find $x_a=0.21$ nm. Hence, the condition (A3) reads $0.13\ \mathrm{nm}<x_m<0.21$ nm. We assume that the minimum positions of both potentials are the same and are equal to $x_m=0.19$ nm. Then, Eq. (A1) yields $A_g=1.6\times10^{18}$ Hz and $A_e=3.17\times10^{18}$ Hz, while Eq. (A2) gives $\alpha_g=\alpha_e=53\ \mathrm{nm}^{-1}$. We recognize that, due to the lack of data and knowledge, the above values may be substantially different from the actual parameters. However, we believe that the difference is not dramatic.

APPENDIX B: DENSITY-MATRIX EQUATIONS FOR A COHERENTLY DRIVEN ATOM

We present the density-matrix equations for a coherently driven atom. We assume that the atom is driven by one or several classical coherent plane-wave fields $\mathbf{E}_l$. Here the index l labels the fields. The set $\{\mathbf{E}_l\}$ may include not only the incident (leftward-propagating) fields but also the reflected (rightward-propagating) ones. For simplicity, we consider the case where all the driving fields propagate perpendicularly to the surface of the dielectric. The expressions for the fields are given by $\mathbf{E}_l=[\mathcal{E}_l e^{i(\beta_l x-\omega_l t)}\boldsymbol{\epsilon}_l+\mathrm{c.c.}]/2$, where $\mathcal{E}_l$, $\boldsymbol{\epsilon}_l$, ω_l, and

$|\beta_l| = \omega_l/c$ are the envelopes, the polarization vectors, the frequencies, and the wave numbers, respectively. The quantities β_l are positive or negative for rightward- or leftward-propagating fields, respectively.

The interaction between the atom and the driving fields is described by the Hamiltonian

$$H_I = -\frac{\hbar}{2}\sum_{lab}(\Omega_{lab}e^{-i\omega_l t}|a\rangle\langle b| + \text{H.c.}), \tag{B1}$$

where

$$\Omega_{lab} = \frac{\mathcal{E}_l d_{leg}}{\hbar}F_{ab}(\beta_l) \tag{B2}$$

is the Rabi frequency for the action of the field $\mathbf{E}_l$ on the transition between the translational levels $|a\rangle$ and $|b\rangle$. Here, $d_{leg} = \boldsymbol{\epsilon}_l \cdot \langle e|\mathbf{d}|g\rangle$ is the projection of the atomic dipole moment onto the polarization vector $\boldsymbol{\epsilon}_l$, and $F_{ab}(k) = \langle \varphi_a|e^{ikx}|\varphi_b\rangle$ is the overlapping matrix element for the transition between the center-of-mass states φ_a and φ_b with a momentum transfer of $\hbar k$. It is interesting to note that, when we use the momentum representations $\tilde{\varphi}_a(p)$ and $\tilde{\varphi}_b(p)$ for the wave functions $\varphi_a(x)$ and $\varphi_b(x)$, respectively, we have

$$F_{ab}(k) = \int_{-\infty}^{\infty}\tilde{\varphi}_a^*(p+\hbar k)\tilde{\varphi}_b(p)dp. \tag{B3}$$

Equation (B3) indicates that the overlapping factor $F_{ab}(k)$ takes into account the change in the momentum of the atom.

When we apply the Schrödinger equation $i\hbar\dot{\rho} = [H_I, \rho]$ to the Hamiltonian (B1) and include the radiative decay terms, described by Eqs. (15), we obtain the following equations for the density matrix ρ of the atom:

$$\dot{\rho}_{aa'} = \frac{i}{2}\sum_{l,b}(\Omega_{lab}\rho^*_{a'b}e^{-i\delta_{lab}t} - \Omega^*_{la'b}\rho_{ab}e^{i\delta_{la'b}t}) - \frac{1}{2}\sum_{a''}(\gamma_{a''a}e^{i\omega_{aa''}t}\rho_{a''a'} + \gamma^*_{a''a'}e^{i\omega_{a''a'}t}\rho_{aa''}),$$

$$\dot{\rho}_{ab} = \frac{i}{2}\sum_{l,b'}\Omega_{lab'}\rho_{b'b}e^{-i\delta_{lab't}} - \frac{i}{2}\sum_{l,a'}\Omega_{la'b}\rho_{aa'}e^{-i\delta_{la'bt}} - \frac{1}{2}\sum_{a'}\gamma_{a'a}e^{i\omega_{aa't}}\rho_{a'b},$$

$$\dot{\rho}_{bb'} = -\frac{i}{2}\sum_{l,a}(\Omega_{lab'}\rho^*_{ab}e^{-i\delta_{lab't}} - \Omega^*_{lab}\rho_{ab'}e^{i\delta_{labt}}) + \frac{1}{2}\sum_{aa'}(\gamma_{aa'bb'} + \gamma^*_{a'ab'b})e^{i(\omega_{bb'}-\omega_{aa'})t}\rho_{aa'}. \tag{B4}$$

Here, $\delta_{lab} = \omega_l - \omega_a + \omega_b$ is the detuning of the driving-field frequency ω_l from the atomic transition frequency ω_{ab}.

We note that Eqs. (B4) do not include the interaction of the atom with the phonons of the solid. We can take into account the decay due to phonons by adding phenomenological terms [36]. The coefficients of such terms are phonon absorption and emission probabilities and can be calculated in second-order perturbation theory [30,31].

[1] V. I. Balykin, K. Hakuta, Fam Le Kien, J. Q. Liang, and M. Morinaga, Phys. Rev. A **70**, 011401(R) (2004); Fam Le Kien, V. I. Balykin, and K. Hakuta, *ibid.* **70**, 063403 (2004).

[2] E. G. Lima, M. Chevrollier, O. Di Lorenzo, P. C. Segundo, and M. Oriá, Phys. Rev. A **62**, 013410 (2000).

[3] T. Passerat de Silans, B. Farias, M. Oriá, and M. Chevrollier, Appl. Phys. B: Lasers Opt. **82**, 367 (2006).

[4] Fam Le Kien, S. Dutta Gupta, V. I. Balykin, and K. Hakuta, Phys. Rev. A **72**, 032509 (2005).

[5] Fam Le Kien, V. I. Balykin, and K. Hakuta, Phys. Rev. A **73**, 013819 (2006).

[6] M. Boustimi, B. Viaris de Lesegno, J. Baudon, J. Robert, and M. Ducloy, Phys. Rev. Lett. **86**, 2766 (2001).

[7] N. Schlosser, G. Reymond, I. Protsenko, and P. Grangier, Nature (London) **411**, 1024 (2001).

[8] S. Kuhr, W. Alt, D. Schrader, M. Müller, V. Gomer, and D. Meschede, Science **293**, 278 (2001).

[9] C. A. Sackett, D. Kielpinski, B. E. King, C. Langer, V. Meyer, C. J. Myatt, M. Rowe, Q. A. Turchette, W. M. Itano, D. J. Wineland, and C. Monroe, Nature (London) **404**, 256 (2000).

[10] R. Folman, P. Kruger, J. Schmiedmayer, J. Denschlag, and C. Henkel, Adv. At., Mol., Opt. Phys. **48**, 263 (2002).

[11] S. Eriksson, M. Trupke, H. F. Powell, D. Sahagun, C. D. J. Sinclair, E. A. Curtis, B. E. Sauer, E. A. Hinds, Z. Moktadir, C. O. Gollasch, and M. Kraft, Eur. Phys. J. D **35**, 135 (2005).

[12] J. M. McGuirk, D. M. Harber, J. M. Obrecht, and E. A. Cornell, Phys. Rev. A **69**, 062905 (2004).

[13] For a review, see K. H. Drexhage, in *Progress in Optics*, Vol. XII, edited by E. Wolf (North-Holland, Amsterdam, 1974), p. 165.

[14] W. Lukosz and R. E. Kunz, Opt. Commun. **20**, 195 (1977).

[15] A. D. McLachlan, Proc. R. Soc. London, Ser. A **271**, 387 (1963); Mol. Phys. **6**, 423 (1963); **7**, 381 (1963); M. J. Mehl and W. L. Schaich, Surf. Sci. **99**, 553 (1980); P. Goy, J. M. Raimond, M. Gross, and S. Haroche, Phys. Rev. Lett. **50**, 1903 (1983).

[16] G. S. Agarwal, Phys. Rev. A **12**, 1475 (1975).

[17] J. M. Wylie and J. E. Sipe, Phys. Rev. A **30**, 1185 (1984).

[18] G. Barton, J. Phys. B **7**, 2134 (1974); E. A. Power and T. Thirunamachandran, Phys. Rev. A **25**, 2473 (1982).

[19] M. S. Tomas, Phys. Rev. A **51**, 2545 (1995).

[20] J.-Y. Courtois, J.-M. Courty, and J. C. Mertz, Phys. Rev. A **53**, 1862 (1996).

[21] K. P. Nayak *et al.* (unpublished).

[22] H. Hoinkes, Rev. Mod. Phys. **52**, 933 (1980).

[23] W. R. Johnson, V. A. Dzuba, U. I. Safronova, and M. S. Safronova, Phys. Rev. A **69**, 022508 (2004).

[24] M. Chevrollier, M. Fichet, M. Oria, G. Rahmat, D. Bloch, and

M. Ducloy, J. Phys. II **2**, 631 (1992).
[25] Information about the van der Waals coefficients of different internal states can also be obtained using Eqs. (37) and (43)–(50) and Table 1 of Ref. [20].
[26] M. A. Bouchiat, J. Guena, Ph. Jacquier, M. Lintz, and A. V. Papoyan, Appl. Phys. B: Lasers Opt. **68**, 1109 (1999); M. Stephens, R. Rhodes, and C. Wieman, J. Appl. Phys. **76**, 3479 (1994).
[27] V. Sandoghdar, C. I. Sukenik, E. A. Hinds, and S. Haroche, Phys. Rev. Lett. **68**, 3432 (1992).
[28] P. Gies and R. R. Gerhardts, Phys. Rev. B **37**, 10020 (1988).
[29] A. O. Caride, G. L. Klimchitskaya, V. M. Mostepanenko, and S. I. Zanette, Phys. Rev. A **71**, 042901 (2005).
[30] C. Henkel and M. Wilkens, Europhys. Lett. **47**, 414 (1999).
[31] Z. W. Gortel, H. J. Kreuzer, and R. Teshima, Phys. Rev. B **22**, 5655 (1980).
[32] J. M. Wylie and J. E. Sipe, Phys. Rev. A **32**, 2030 (1985).
[33] H. Failache, S. Saltiel, A. Fischer, D. Bloch, and M. Ducloy, Phys. Rev. Lett. **88**, 243603 (2002).
[34] O. Di Stefano, S. Savasta, and R. Girlanda, Phys. Rev. A **61**, 023803 (2000).
[35] L. Allen and J. H. Eberly, *Optical Resonance and Two-Level Atoms* (Dover, New York, 1987).
[36] See, for example, R. W. Boyd, *Nonlinear Optics* (Academic, New York, 1992).
[37] S. Chang and V. Minogin, Phys. Rep. **365**, 65 (2002).